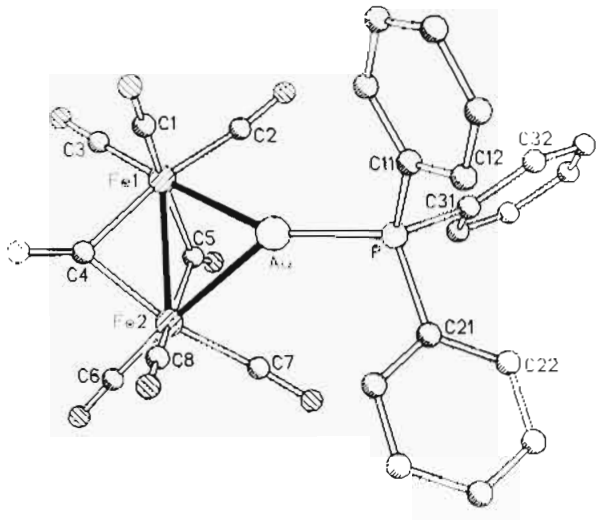

Figure 1. Molecular structure and atom-numbering scheme of the $[Fe_2(CO)_8(\mu\text{-}AuPPh_3)]^-$ anion.

distances are in the range 2.659–2.717 Å (the average of nine experimental distances is 2.68 (2) Å). Two carbonyl ligands also bridge the two iron atoms, the Fe–Fe distance of 2.605 (2) Å being midway between that found in the $[HFe_2(CO)_8]^-$ (2.521 (1) Å)[7] and its parent $[Fe_2(CO)_8]^{2-}$ (2.787 (2) Å).[10] It should be noted that the coordination about Fe is not strictly octahedral, since the terminal carbonyl groups are not collinear with the bridging atoms; e.g., C(1)–Fe(1)–C(5) = 160.1 (4)°. The bridging CO groups are situated closer to the Fe–Fe bond than they would be if the angles were 180°. A similar feature was observed in the species $[HFe_2(CO)_8]^-$[7] and $[Fe_2(CO)_9]$.[11]

Acknowledgment. Financial support of this work was generously provided by CICYT (Spain) (Project PB84-0920) and by the Fonds der Chemischen Industrie (Frankfurt, West Germany). X-ray intensity measurements were carried out at the Institut fur Anorganische Chemie, University of Göttingen, West Germany.

Registry No. **1**, 123752-66-9; $[ClAuPPh_3]$, 14243-64-2; $(Et_4N)_2[Fe_2(CO)_8]$, 26024-88-4; Fe, 7439-89-6; Au, 7440-57-5.

Supplementary Material Available: Tables of all bond distances and angles (Table S1), hydrogen atom coordinates and isotropic displacement parameters (Table S2), and anisotropic thermal parameters (Table S3) (4 pages); a listing of structure factors (Table S4) (21 pages). Ordering information is given on any current masthead page.

(10) Chin, H. B.; Smith, M. B.; Wilson, R. D.; Bau, R. *J. Am. Chem. Soc.* **1974**, *96*, 5285.
(11) Cotton, F. A.; Troup, J. M. *J. Chem. Soc., Dalton Trans.* **1974**, 800.

Contribution from the Scheikundig Laboratorium der Vrije Universiteit, De Boelelaan 1083, Amsterdam 1081 HV, The Netherlands

Model Systems for Initial Stages in Oxidative-Addition Reactions. Theoretical Investigation of η^1 and η^2 Coordination of F_2 and H_2 to $PtCl_4^{2-}$ and $Cr(CO)_5$

F. M. Bickelhaupt, E. J. Baerends,* and W. Ravenek

Received May 16, 1989

There is considerable interest in the bonding of dihalogens and H_2 to transition metals, because of its relevance to homogeneous catalysis and because X_2 complexes (X = H, halogen) may serve as models for intermediates formed during early stages of oxidative-addition reactions.[1-3] Van Koten et al.[1] reported the first

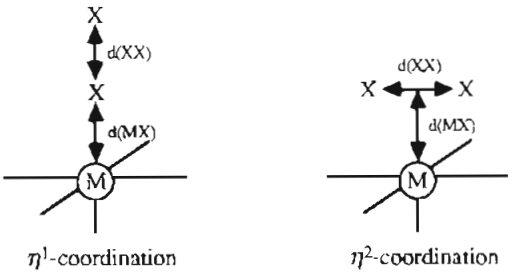

Figure 1. Geometry parameters d(M–X) and d(X–X). For all Pt complexes, first-order relativistic effects[21] are taken into account in determining the optimum geometry. However, the analysis of the bonding mechanism (see tables) is purely nonrelativistic.

example of a complex in which the highly reactive halogen I_2 is coordinated to a transition metal. They synthesized the square-pyramidal organoplatinum(II) compound $[Pt^{II}\{C_6H_3(CH_2NMe_2)\text{-}o,o'\}(\eta^1\text{-}I_2)]$ (**1**), in which the iodine molecule interacts with the platinum d^8 center in the η^1-coordination mode.

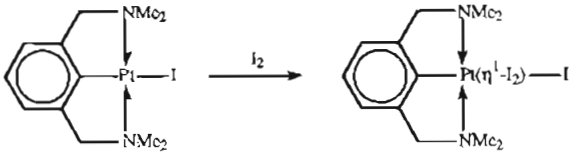

2 **1**

In this work we present the first theoretical study of η^1 coordination of X_2 to a d^8 Pt center, using a density-functional MO–LCAO method commonly referred to as the Hartree–Fock–Slater (HFS) method.[4-8] The purpose of this study is to understand why I_2 coordinates in a monohapto fashion to $[Pt^{II}\{C_6H_3(CH_2NMe_2)_2\text{-}o,o'\}]$ (**2**). We present results of HFS calculations on the model complex $PtCl_4^{2-}$ (D_{4h} symmetry) (**3**) and the monohapto (**4**) and dihapto (**5**) complexes of **3** with F_2. The nodal

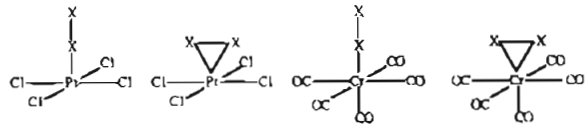

X = F	**4**	**5**	**9**	**10**
X = H	**6**	**7**	**11**	**12**

structure of the frontier orbitals ($3\sigma_u$ (σ^*) of F_2 and $2e_{1g}$ (Pt $5d_\pi$–Cl $3p_\pi$) of $PtCl_4^{2-}$) is shown to play a key role in determining the preference for end-on coordination. As will be explained, it is important for the stability of a complex such as **1** that the platinum d^8 center is embedded in a rigid square-planar structure that (in good approximation) keeps its geometry fixed[1] as the iodine coordinates to it. In contrast to the η^1 coordination found in **1**, it is known that H_2 coordinates side-on to $Cr(CO)_5$. For a better understanding of the factors that influence the bonding in **1** and for comparison with the literature,[9-11] calculations are

(1) Van Beek, J. A. M.; Van Koten, G.; Smeets, W. J. J.; Spek, A. L. *J. Am. Chem. Soc.* **1986**, *108*, 5010.
(2) Andréa, R. R.; Vuurman, M. A.; Stufkens, D. J.; Oskam, A. *Recl. Trav. Chim. Pays-Bas* **1986**, *105*, 372.
(3) Upmacis, R. K.; Gadd, G. E.; Poliakoff, M.; Simpson, M. B.; Turner, J. J.; Whyman, R.; Simpson, A. F. *J. Chem. Soc., Chem. Commun.* **1985**, 27.
(4) Slater, J. C. *Quantum Theory of Molecules and Solids*; McGraw-Hill: New York, 1974; Vol. 4.
(5) Baerends, E. J.; Ellis, D. E.; Ros, P. *Chem. Phys.* **1973**, *2*, 41.
(6) Baerends, E. J.; Ros, P. *Chem. Phys.* **1973**, *2*, 52.
(7) Baerends, E. J.; Ros, P. *Chem. Phys.* **1975**, *8*, 412.
(8) Heijser, W.; Van Kessel, A. Th.; Baerends, E. J. *Chem. Phys.* **1976**, *16*, 371.
(9) Saillard, J.-Y.; Hoffmann, R. *J. Am. Chem. Soc.* **1984**, *106*, 2006.
(10) Hay, P. J. *Chem. Phys. Lett.* **1984**, *103*, 466.
(11) Hay, P. J. *J. Am. Chem. Soc.* **1987**, *109*, 705.

0020-1669/90/1329-0350$02.50/0

Table I. Overlaps, Energies, and Populations for $Cr(CO)_5(\eta^1$- and η^2-$H_2)$[a]

	η^1	η^2
	Geometry (Å)	
$d(Cr-H_2)$	1.85	1.68
$d(H-H)$	0.77	0.87
	Overlaps $\langle H_2 \vert Cr(CO)_5\rangle$	
$\langle 1\sigma_g \vert 8a_1\rangle$	0.35	0.48
$\langle 1\sigma_u \vert 8a_1\rangle$	0.25	
$\langle 1\sigma_u \vert 7e_1\text{-}x\rangle$		0.23
	Populations (e)	
$P(1\sigma_u)$	−0.02	0.09
$P(1\sigma_g)$	1.77	1.63
$P(8a_1)$	0.16	0.30
$P(7e_1\text{-}x)$	2.00	1.90
	Energies (eV)	
ΔE_σ	−0.61	−1.14
ΔE_π	−0.03	−0.50
ΔE_{rest}	0.00	−0.04
ΔE_{oi}[b]	−0.64	−1.68
$\Delta E°$	+0.82	+1.34
$\Delta E(H\leftrightarrow H)$	0.00	+0.13
ΔE_{tot}	+0.18	−0.21

[a] $P(\varphi)$ is the gross Mulliken population that the fragment-orbital φ acquires in the complex. ΔE_σ refers to orbital interactions in A_1 symmetry; ΔE_π refers to orbital interactions in E symmetry (η^1,C_{4v}) and B_1 symmetry (η^2,C_{2v}), respectively. $\Delta E°$ is the steric repulsion that comprises both the four-electron destabilizing interactions between occupied orbitals ("exchange repulsion") and the electrostatic interaction between the electronic and nuclear charge distributions of the fragments. $\Delta E(H\leftrightarrow H)$ is the energy required to stretch the H–H distance from the value of the free diatomic to the value in the complex. [b] oi = orbital interaction.

performed on the monohapto and dihapto complexes of the C_{4v} symmetric $Cr(CO)_5$ (**8**) with H_2 (**11**, **12**). Finally, monohapto and dihapto complexes of $PtCl_4^{2-}$ with H_2 (**6** and **7**, respectively) and of F_2 with $Cr(CO)_5$ (**9** and **10**, respectively) are briefly considered.

Method

The MOs are expanded in a large basis set of Slater type orbitals (STOs). The basis is of triple-ζ quality (three STOs per *nl* shell) for Cr, Pt, F, and H. A 3d polarization function has been added on F, and polarization functions of *n*p type have been added to Cr, Pt, and H. The ligands CO and Cl are described with double-ζ bases. For all atoms (except H) we apply the frozen-core (FC) approximation.[5] The geometries of **3**[12] and **8**[13] are taken from the literature and are kept fixed: **3**, $d(PtCl) = 2.31$ Å, $\angle(ClPtCl) = 90°$, D_{4h} symmetry; **8**, $d(CrC) = 1.91$ Å, $d(CO) = 1.14$ Å, $\angle(CrCO) = 180°$, $\angle(CCrC) = 90°$, C_{4v} symmetry. The geometries of **4**–**7** and **9**–**12** are characterized by the distances $d(MX)$ and $d(XX)$ (Figure 1), which have been optimized in a number of cases (see text and tables). Geometry optimizations have been carried out with the simple Xα exchange-correlation potential.[4] As the pure Xα energies are too strongly bonding, the energy data reported have been obtained in the optimum geometry with more sophisticated density functionals for exchange and correlation. Exchange is described with Slater's $\rho^{1/3}$ potential (Xα with $\alpha = {}^2/_3$), with a nonlocal correction due to Becke.[14-16] According to the suggestion by Stoll et al.[17] only correlation between electrons of different spin is introduced, for which electron gas data (in the Vosko–Wilk–Nusair[18] parametrization) are used. Considerable experience shows that with this approach metal–ligand interaction energies are described to an accuracy of a few tenths of an electronvolt (in the order of 5 kcal/mol).[19,20] As shown recently by Becke,[15] the gradient corrections in general lead, apart from the significant reduction in bond strength, to slight bond lengthening.

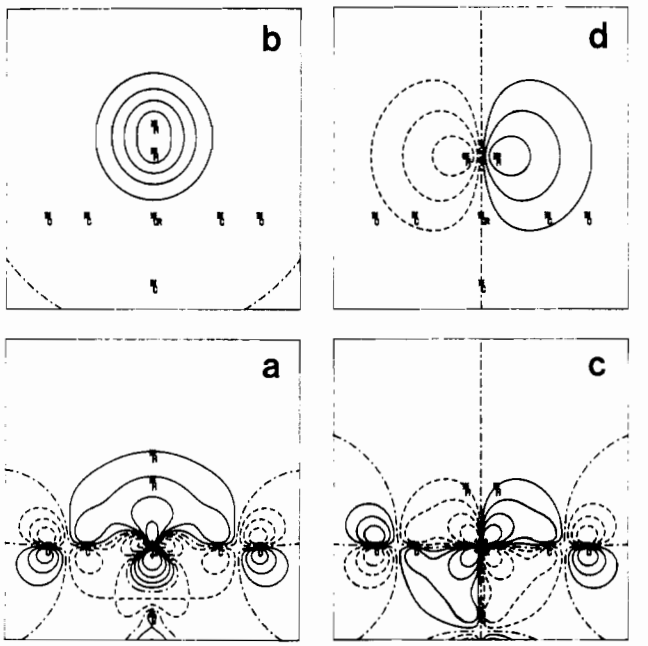

Figure 2. Frontier orbitals of $Cr(CO)_5$ and H_2: (a) $Cr(CO)_5$ LUMO, $8a_1$; (b) H_2 HOMO, $1\sigma_g$; (c) $Cr(CO)_5$ HOMO, $7e_1$; (d) H_2 LUMO, $1\sigma_u$. Note that in each orbital plot the positions of the nuclei of the other fragment are indicated.

Results and Discussion

We first present in Table I the results of a population and bonding energy analysis of $Cr(CO)_5(\eta^1$- and η^2-$H_2)$, using the Xα-optimized Cr–H and H–H distances. The main contribution to the coordinative bond has been believed to be σ-donation out of the H_2 $1\sigma_g$ into the $8a_1$ LUMO of $Cr(CO)_5$ (a dsp hybrid that derives from the $3d_{z^2}$ (e_g) orbital of the parent octahedral $Cr(CO)_6$ molecule; see ref 3, 22, 23). The orbital plot (Figure 2a) shows a large contribution of equatorial CO π^* to this orbital. As the π^* interacts with the 3d in this orbital in a bonding (in-phase) fashion, the positive lobe of the $8a_1$ is quite extended, yielding large overlaps with a ligand donor orbital such as H_2 $1\sigma_g$ (see below). A second contribution to the coordinative bond may come from back-donation into the high-lying unoccupied σ^* orbital ($1\sigma_u$) of H_2. This orbital may, in η^2 coordination, act as an acceptor orbital for π-back-donation out of the $Cr(CO)_5$ HOMO (the $7e_1$, a $3d_\pi$ orbital with respect to the Cr–H_2 bond axis). This interaction is probably rather weak, due to the high energy of the σ^*, but is still believed to determine the preference of H_2 for η^2 coordination. This would fit in with the orientation of H_2 parallel to the PR_3–W–PR_3 axis in the η^2 complex $W(CO)_3(PR_3)_2H_2$:[10,11,24] the d_π interacting with the equatorial CO's is more stabilized (by the CO π^* orbitals) than the other d_π in the plane of the PR_3 ligands and is therefore less suitable for π-back-bonding to the H_2 σ^*. Saillard and Hoffmann[9] infer from their extended Hückel calculations that there is a "strong interaction" of $3d_\pi$ with σ^* of η^2-H_2. Andrêa et al.[2] have argued, from an analysis of CO vibration energies, that the back-bonding interaction to H_2 might even be much stronger than inferred from the calculations by Saillard and Hoffmann[9] and Hay.[10,11]

(12) Carsey, T. P.; Boudreaux, E. A. *Theoret. Chim. Acta* **1980**, *56*, 211.
(13) Rozendaal, A. Thesis, Vrije Universiteit, Amsterdam, 1985, p 103.
(14) Becke, A. D. *Int. J. Quantum Chem.* **1983**, *23*, 1915.
(15) Becke, A. D. In *The Challenge of d and f Electrons*; Salahub, D. R.; Zerner, M. C., Eds.; ACS Symposium Series 394; American Chemical Society: Washington, DC, 1989; p 165.
(16) Ziegler, T.; Tschinke, V.; Becke, A. *Polyhedron* **1987**, *6*, 685.
(17) Stoll, H.; Golka, E.; Preus, H. *Theoret. Chim. Acta* **1980**, *55*, 29.
(18) Vosko, S. H.; Wilk, L.; Nusair, M. *Can. J. Phys.* **1980**, *58*, 1200.
(19) Ziegler, T.; Tschinke, V.; Ursenbach, C. *J. Am. Chem. Soc.* **1987**, *109*, 4825.
(20) Ziegler, T.; Tschinke, V.; Versluis, L.; Baerends, E. J. *Polyhedron* **1988**, *7*, 1625.
(21) Ziegler, T.; Snijders, J. G.; Baerends, E. J. *J. Chem. Phys.* **1981**, *74*, 1271.
(22) Hoffmann, R.; Chen, M. M. L.; Elian, M.; Rossi, A. R.; Mingos, D. M. P. *Inorg. Chem.* **1974**, *13*, 2666.
(23) Heijser, W.; Baerends, E. J.; Ros, P. *Faraday Symp.* **1980**, *14*, 211.
(24) Kubas, G. J.; Ryan, R. R.; Swanson, B. I.; Vergamini, P. J.; Wasserman, H. J. *J. Am. Chem. Soc.* **1984**, *106*, 451.

In order to answer these questions, we have explicitly split up the total bond energy according to the irreducible representations in which the orbital interactions occur (cf. ref 25–27). Let us first discuss the σ bond, which occurs in A_1 symmetry both in η^1 and η^2 coordination. As shown in Table I, the overlap of the $1\sigma_g$ with the $8a_1$ is even considerably larger for η^2 coordination. This is understandable from the shape of the $8a_1$, which, as pointed out before, has a broad positive lobe extending over the C atoms of the equatorial CO's. It is therefore well suited for overlap with a side-on-approaching $1\sigma_g$. We calculate indeed, contrary to the suggestion by Saillard and Hoffmann,[9] the σ-bond strength to be much stronger (by 0.53 eV) in the η^2 mode compared to η^1. This is also reflected in the much larger σ donation out of the $1\sigma_g$ into the $8a_1$ ($P(1\sigma_g) = 1.63$ for η^2 with respect to 1.77 for η^1, with populations of 0.30 and 0.16, respectively, in the $Cr(CO)_5$ LUMO $8a_1$). In the end-on coordination there may also be a contribution to the σ bond from the H_2 σ^*. This contribution cannot be revealed by our symmetry-based analysis but is expected to be very weak as there is not a high-energy σ-donor orbital in the $Cr(CO)_5$ fragment. This expectation is borne out by the negligible population of the σ^* (−0.02 e). As a matter of fact, the total σ bond is so weak—and there is no π bond in end-on coordination—that the steric repulsion (the four-electron destabilizing interactions between occupied orbitals) predominates, with net antibonding as a result. [N.B. The Cr–H distance has been determined from pure Xα calculations, which do yield slight bonding, but obviously this distance, although reasonable, has no particular significance.]

Turning now to the π bond, which is formed by a metal $3d_\pi/H_2$ σ^* interaction in the η^2 mode, we note that this interaction occurs in B_1 symmetry in the C_{2v} group of the η^2 complex. The π-bond energy is calculated to be substantial: 0.50 eV. The presence of a π bond in side-on coordination therefore is an important factor in favor of this coordination mode. In summary, then, our calculations indicate the expected preference for η^2 coordination, but the reason is 2-fold: the calculated σ- and π-bond energies show that this preference arises from both a significant π-back-bonding contribution *and* a considerably larger σ-bond strength in the η^2 mode. The much stronger interaction between metal fragment and η^2-H_2 is reflected in the longer calculated H–H bond (0.87 versus 0.77 Å). Of course, both the donation from the bonding $1\sigma_g$ and the back-donation into the antibonding $1\sigma_u$ weaken the H–H bond.

In theoretical studies of oxidative addition[28–30] to metal fragments with HOMOs and LUMOs similar to those of $Cr(CO)_5$ (such as $Pt(PH_3)_2$), a side-on approach of H_2 has been taken as the initial stage of the reaction. This fits in perfectly with the bonding picture given above. It may therefore come as a surprise at first sight that the approach of a dihalogen, also with a σ^*-acceptor orbital, to a metal fragment with a high-lying d_π-donor orbital would be end-on, as suggested by the synthesis of **1**. We have carried out calculations on the η^1 and η^2 coordination of F_2 to $PtCl_4^{2-}$, as a model system for **1**. In dihalogens the LUMO is a σ^* (the $3\sigma_u$ in F_2) that is at extremely low energy compared to the $H_2\sigma^*$ (we compute it more stable by 6.8 eV!) and even compared to the acceptor orbital in well-known π acids such as CO. This has several origins. The atomic orbitals of F are at low energy and are contracted due to the high nuclear charge. The bond length in F_2 is large due to the repulsion between the p_π lone pairs on the two atoms, so the (contracted) AOs overlap little and the total spread in bonding and antibonding 2p-derived MOs is not very large; i.e., the antibonding combination of the p_σ AOs (the $3\sigma_u$) is not much destabilized. Figure 3 gives a picture of this orbital, which clearly shows its p_σ–p_σ character. The metal fragment, $PtCl_4^{2-}$, has a well-known orbital pattern: there are four fairly close-lying occupied 5d orbitals, the highest being the $5d_\pi$ set $2e_{1g}$, the lowest the $5d_\sigma$ (=$5d_{z^2}$, $3a_{1g}$). The in-plane $5d_{xy}$ is between, and the LUMO is the in-plane $5d_{x^2-y^2}$. Both because of the high energy of the 5d orbitals, which are being pushed up by the antibonding interaction with the Cl 3p's (note also the negative charge on the metal fragment), and because of the poor overlap of $5d_{x^2-y^2}$ with incoming ligands, we expect $PtCl_4^{2-}$ to be a good donor and a poor acceptor. It can act as a π donor through

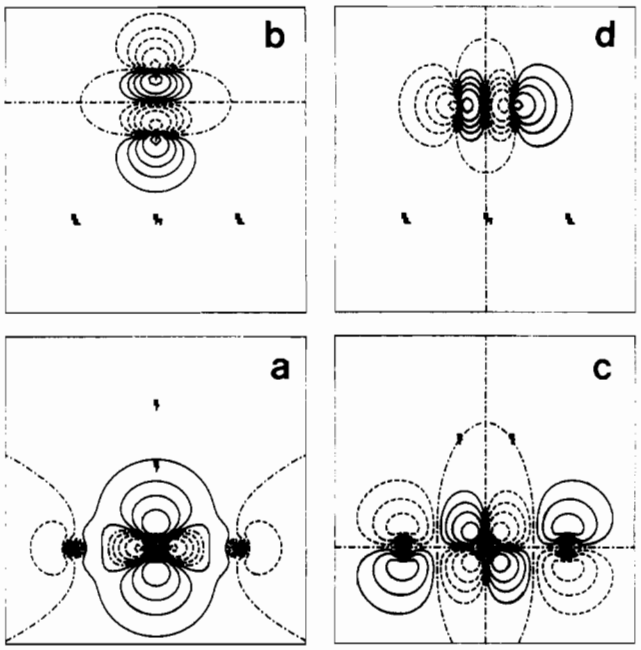

Figure 3. Frontier orbitals of $PtCl_4^{2-}$ and F_2: (a) $PtCl_4^{2-}$ σ-donor orbital $3a_{1g}$ ($5d_{z^2}$); (b) η^1-F_2 LUMO, $3\sigma_u$; (c) $PtCl_4^{2-}$ π-donor HOMO, $2e_{1g}$; (d) η^2-F_2 LUMO, $3\sigma_u$.

Table II. Overlaps, Populations, and Energies for $PtCl_4^{2-}$(η^1- and η^2-F_2)[a]

	η^1	η^2
	Geometry (Å)	
d(Pt–F_2)	2.31	3.05
d(F–F)	1.70	1.48[b]
	Overlaps $\langle F_2 \vert PtCl_4^{2-}\rangle$	
$\langle 3\sigma_u \vert 3a_{1g}\rangle$	0.11	
$\langle 3\sigma_u \vert 2e_{1g}\text{-}x\rangle$		0.02
	Populations (e)	
$P(3\sigma_u)$	0.65	0.36
$P(3a_{1g})$	1.41	2.00
$P(2e_{1g}\text{-}x)$	2.00	1.64
	Energies (eV)	
ΔE_σ	−3.66	−0.16
ΔE_π	−0.12	−0.77
ΔE_{rest}	−0.12	−0.08
ΔE_{oi}[c]	−3.90	−1.00
$\Delta E°$	+1.21	+0.23
ΔE(F↔F)	+0.97	+0.09
ΔE_{tot}	−1.72	−0.68

[a] See Table I for explanation of the entries. [b] The F–F distance in η^2 coordination has been chosen slightly longer than in free F_2; it has not been optimized. [c] oi = orbital interaction.

(25) Ziegler, T.; Rauk, A. *Theoret. Chim. Acta* **1977**, *46*, 1.
(26) Ziegler, T.; Rauk, A. *Inorg. Chem.* **1979**, *18*, 1755.
(27) Baerends, E. J.; Rozendaal, A. In *Quantum Chemistry: The Challenge of Transition Metals and Coordination Chemistry*; Veillard, A., Ed.; D. Reidel: Dordrecht, The Netherlands, 1986, p 159.
(28) Low, J. J.; Goddard, W. A., III *J. Am. Chem. Soc.* **1984**, *106*, 6928.
(29) Noell, J. O.; Hay, P. J. *J. Am. Chem. Soc.* **1982**, *104*, 4578.
(30) Kitaura, K.; Obara, S.; Morokuma, K. *J. Am. Chem. Soc.* **1981**, *103*, 2891.

the $2e_{1g}$ and as a σ donor through the $3a_{1g}$ (these orbitals are plotted in Figure 3). In Table II we present the population and energy analysis of the $PtCl_4^{2-}$–F_2 interaction. Considering the σ (A_1) bond energy first, we note that the situation is strikingly different from that of $Cr(CO)_5$–H_2. The σ interaction is much stronger now in η^1 coordination than in η^2 coordination. This is to be expected. In η^1 coordination the metal $5d_{z^2}$ is able to donate electrons into the F_2 $3\sigma_u$ orbital; i.e., the metal can act as donor, for which it is predestined by the Cl ligands, and the F_2 can act as acceptor, for which it has an extremely low-lying LUMO available: a strong σ bond of 3.7 eV results. This is a clear case of *σ back-donation*. In η^2 coordination the only possibility for σ bonding is σ donation out of occupied F_2 orbitals such as $1\pi_u$ and $3\sigma_g$ (the σ^* orbital cannot act as a σ acceptor in this coordination mode). But these orbitals are too low in energy, and there is not a good acceptor orbital present on the metal fragment: a small σ bond of 0.16 eV is the result.

Looking next at the π bond, we note that there is in η^1 coordination no possibility for π-type orbital interaction. However, one would expect a quite strong π bond in η^2 coordination because the $3\sigma_u$ of F_2 should now act as a good π acceptor for the donor $5d_\pi$ ($2e_{1g}$) HOMO of $PtCl_4^{2-}$. In fact, however, the π-bond energy is only 0.8 eV, much less than the 3.7 eV of the σ bond (also by the $3\sigma_u$) in η^1 coordination. The explanation is provided by the much smaller overlap of $3\sigma_u$ with the $2e_{1g}$ ($5d_\pi$) than with the $3a_{1g}$ ($5d_{z^2}$): 0.02 versus 0.11 (see Table II). The reason for this difference is clear from the plots of Figure 3. The antibonding character of the Pt $5d_\pi$/Cl $3p_\pi$ interaction in the $2e_{1g}$ causes nodal surfaces between Pt and the ligands, which intersect the lobes of the F_2 $3\sigma_u$. Moreover, the $3\sigma_u$ itself has nodal surfaces that cut through the lobes of the $5d_\pi$, so there is extensive cancellation of positive and negative contributions to the $2e_{1g}/3\sigma_u$ overlap, with a quite small net overlap of 0.02 as a result. Because of the lack of good π interaction with the $3\sigma_u$ in the η^2 coordination and the presence of a good σ interaction with this orbital in the η^1 mode, there is an unequivocal preference for η^1 coordination. The η^1 interaction between F_2 and the metal fragment leads to a large population of the $3\sigma_u$ ($P(3\sigma_u) = 0.65$) and a considerable lengthening of the bond.

Our findings for the $PtCl_4^{2-}$–F_2 system are in agreement with the experimental observation made for **1**. Two important differences between **1** and our model system are the longer bond length of I_2 and the different ligands surrounding Pt. We have carried out one calculation with I_2, taking for the η^1 mode the geometry from ref 1 and for η^2 distances that differ from η^1 in the same way as in $PtCl_4^{2-}$–F_2 (d(Pt–I_2) = 3.64 Å, d(I–I) = 2.70 Å). These calculations yield a picture for bonding to I_2 that is completely analogous to the one for F_2. The overlap of the I_2 σ^* with the $2e_{1g}$ in the η^2 mode is only 0.03, which is to be compared to an overlap of 0.17 of the σ^* with $3a_{1g}$ ($5d_{z^2}$) in the η^1 mode; these overlaps are not very sensitive to geometry variation. Correspondingly, we obtain total bonding energies of 0.35 eV for η^2 and 1.27 eV for η^1. Evidently the nodal structure of the frontier orbitals makes the η^2 bonding comparatively weak also in the case of I_2. Concerning the Cl^- ligands in our model substrate, we note that the negative charge on $PtCl_4^{2-}$, compared to the neutrality of the metal fragment in **1**, will relatively destabilize the metal d levels, although the levels of the approaching F_2 will also shift upward. $PtCl_4^{2-}$ is therefore expected to back-donate more readily than the metal fragment in **1**, both in the η^1 and η^2 modes. The bond strength may therefore be smaller in **1**, but the arguments for the preference for η^1 should still hold.

It probably is not accidental that the synthesized η^1 complex **1** has a rigid square-planar structure. We have not embarked upon calculations of the possible reaction path to full oxidative addition, but it is clear that here as in the cases of H_2 interacting with $Pt(PH_3)_2$[28-30] and with the Wilkinson catalyst $Rh(PR_3)_3Cl$[31,32] the bending back of the ligands would be an important factor in stabilizing possible η^2 intermediates. In case the oxidative addition proceeds via an η^2 intermediate, bending back two trans Cl ligands in $PtCl_4^{2-}$ would cause the ligands, now entering the 5d lobes, to change from π pushers into more effective σ pushers. This destabilization of the $5d_\pi$ is a well-known effect; it is observed in the quoted examples. Thus, bending would make the $5d_\pi$ more effective for π bonding to a side-on X_2 and would assist the X–X dissociation. Of course, these remarks should not be interpreted as implying that the oxidative addition of a dihalogen will necessarily proceed via an η^2 intermediate; an alternative to be considered, for instance, is the breaking of the X–X bond in the η^1 complex.

Table III. Overlaps, Populations, and Energies for $Cr(CO)_5$(η^1- and η^2-F_2)[a]

	η^1	η^2
	Geometry (Å)	
d(Cr–F_2)	2.43	2.26
d(F–F)	1.42	1.48[b]
	Overlaps $\langle F_2 \vert Cr(CO)_5 \rangle$	
$\langle 3\sigma_g \vert 8a_1 \rangle$	0.13	0.05
$\langle 3\sigma_u \vert 8a_1 \rangle$	0.13	
$\langle 1\pi_u \vert 8a_1 \rangle$		0.17
$\langle 3\sigma_u \vert 7e_1\text{-}x \rangle$		0.03
	Populations (e)	
$P(3\sigma_g)$	1.97	2.00
$P(3\sigma_u)$	0.01	0.39
$P(1\pi_u)$	2.00	1.92
$P(8a_1)$	0.01	0.07
$P(7e_1\text{-}x)$	2.00	1.66
	Energies (eV)	
ΔE_σ	−0.23	−0.38
ΔE_π	−0.05	−0.81
ΔE_{rest}	−0.00	−0.05
ΔE_{oi}[c]	−0.28	−1.24
ΔE^o	+0.51	+1.31
ΔE(F↔F)	+0.00	+0.09
ΔE_{tot}	+0.23	+0.08

[a] See Table I for explanation of the entries. [b] The F–F distance has not been optimized in the η^2 mode. [c] oi = orbital interaction.

For completeness we have also considered the more academic cases of F_2 interacting with $Cr(CO)_5$ and of H_2 interacting with $PtCl_4^{2-}$. Considering $Cr(CO)_5$–F_2 first (Table III), we note that the main difference with $PtCl_4^{2-}$–F_2 is for σ interactions: $Cr(CO)_5$ is a good σ acceptor, whereas $PtCl_4^{2-}$ is a good σ donor. The σ-acceptor property of $Cr(CO)_5$ is however not very important, since F_2 is a very poor donor anyway. Neither in end-on nor in side-on coordination is there significant σ donation into the metal $8a_1$ (cf. the populations of 0.01 and 0.07 e in Table III). The σ donation in η^2 mode is from the $1\pi_u$ orbital of F_2 (cf. the Dewar–Chatt–Duncanson bonding of ethylene to metal centers), which has higher energy than $3\sigma_g$ and a better overlap with $8a_1$ (see the table). The corresponding σ-bonding energies are small, although obviously the good acceptor property of the $8a_1$ does show up, in η^2 mode, in a larger ΔE_σ than that with $PtCl_4^{2-}$: −0.38 versus −0.16 eV. For η^2 coordination we have the possibility of π back-donation out of the $3d_\pi$ ($7e_1$) HOMO into the $3\sigma_u$, but the $Cr(CO)_5$ $3d_\pi$ is at lower energy than $PtCl_4^{2-}$ $5d_\pi$, as it is pushed down by the bonding mixing of CO π^* orbitals instead of being pushed up by antibonding mixing of Cl 3p. The overlap with $3\sigma_u$ is however slightly better as the $7e_1$ does not change phase between metal and equatorial ligand. Still, the nodes in the $3\sigma_u$ prevent the building up of a large overlap. The net effect is a very similar ΔE_π, ~0.8 eV, in both cases. The absence of a good σ bond in the end-on coordination to $Cr(CO)_5$ implies however that this ΔE_π is sufficient to make the η^2 coordination more favorable, or rather less unfavorable: there still is slight net antibonding.

(31) Dedieu, A.; Strich, A. *Inorg. Chem.* **1979**, *18*, 2940.
(32) Dedieu, A. *Inorg. Chem.* **1980**, *19*, 375.

Table IV. Overlaps, Populations, and Energies for $PtCl_4^{2-}$(η^1- and η^2-H_2)[a]

	η^1	η^2
	Geometry	
d(Pt-H_2)	2.95	2.82
d(H-H)	0.89[b]	0.89[b]
	Overlaps	
$\langle 1\sigma_u \vert 3a_{1g}\rangle$	0.22	
$\langle 1\sigma_u \vert 2e_{1g}\text{-}x\rangle$		0.05
$\langle 1\sigma_g \vert 3a_{1g}\rangle$	0.09[5]	0.16
	Populations (e)	
$P(1\sigma_u)$	0.08	0.02
$P(1\sigma_g)$	1.99	2.01
$P(3a_{1g})$	1.97	2.01
$P(2e_{1g}\text{-}x)$	2.00	1.99
	Energies (eV)	
ΔE_σ	-0.23	-0.19
ΔE_π	-0.07[5]	-0.07
ΔE_{rest}	-0.05	-0.06
ΔE_{oi}[c]	-0.36	-0.31
$\Delta E°$	+0.00	+0.25[5]
ΔE(H↔H)	+0.16	+0.16
ΔE_{tot}	-0.19	+0.10

[a] See Table I for explanation of the entries. [b] The H-H distances have not been optimized. [c] oi = orbital interaction.

The interaction of H_2 with $PtCl_4^{2-}$ is very weak, as expected: -0.19 eV in the η^1 mode and +0.10 eV in the η^2 mode (Table IV). The overlap of the d_σ ($3a_{1g}$) with H_2 σ^* is a sizable 0.22 in the η^1 mode, but the high energy of σ^* prevents strong σ bonding: $\Delta E_\sigma = -0.23$ eV, and $P(\sigma^*) = 0.08$ e. In η^2 mode the σ^* could act as π-acceptor orbital, but the overlap of σ^* with $2e_{1g}$ is small (0.05). As there are no nodes in the σ^* (except for the central plane of course), this small overlap must be caused by the different phases of $2e_{1g}$ on Pt and Cl. Although the $Cr(CO)_5$-F_2 example above shows that the mere presence of the nodal planes in the $3\sigma_u$ of η^2-F_2 is sufficient to cause a small overlap with a metal fragment orbital, the case of $PtCl_4^{2-}$-H_2 shows that also nodes in the metal fragment orbital prevent the building up of a large overlap. The small overlap and the high energy of the H_2 σ^* orbital result in a π bond that is quite weak (-0.07 eV). The occupied $1\sigma_g$ of H_2 has a four-electron destabilizing interaction (steric repulsion) with the $PtCl_4^{2-}$ $3a_{1g}$, which cancels in η^2 coordination (larger $1\sigma_g$-$3a_{1g}$ overlap) much of the bonding contributions. In conclusion, H_2 bonds preferentially in η^1 mode to $PtCl_4^{2-}$, as F_2 does, but rather weakly.

Summarizing, we have found the nodal structure of both the F_2 acceptor orbital $3\sigma_u$ (antibonding p_σ-p_σ) and the metal fragment donor orbital $2e_{1g}$ (antibonding $5d_\pi$-Cl 3p) to be responsible for the lack of π bonding in η^2 coordination and therefore for the preference of end-on over side-on coordination of F_2 to $PtCl_4^{2-}$. On the other hand, we have found the extended nature of the $8a_1$ (bonding dsp hybrid + CO π^*) an important factor for the preference of side-on coordination of H_2 to $Cr(CO)_5$. The opposite effects we have found here for on the one hand the π^* orbitals of the CO ligands in $Cr(CO)_5$, combining in a bonding fashion with the metal $3d_\pi$, and on the other hand the $3p_\pi$ orbitals of the Cl ligands in $PtCl_4^{2-}$, combining in an antibonding fashion with the metal $5d_\pi$, once more highlight the important role of ligands in tailoring metal d AOs for particular interactions. It is interesting to note that the η^1-coordinated $PtCl_4^{2-}$-F_2 provides a clear example of a metal-ligand bond that derives its strength from σ *back-donation* from metal to ligand.

Acknowledgment. We wish to thank Prof. G. van Koten for stimulating our interest in the subject of this investigation. The help of P. Vernooijs with the calculations and figures is also gratefully acknowledged.

Registry No. F_2, 7782-41-4; $PtCl_4^{2-}$, 13965-91-8; H_2, 1333-74-0; $Cr(CO)_5$, 26319-33-5.

Contribution from the Departments of Chemistry, Faculty of Science, Shimane University, Matsue 690, Japan, and College of General Education, Osaka University, Osaka 560, Japan

Photoreduction of Methylviologen Catalyzed by Phthalocyanine Complexes of Yttrium(III) and Lanthanoid(III) Metals

Kuninobu Kasuga,*,† Seiji Takahashi,† Keiichi Tsukahara,†,‡ and Takeshi Ohno§

Received February 22, 1989

Photoinduced hydrogen evolution from water has received considerable attention for the storage of solar energy and its conversion into a chemical form. Metal complexes such as $[Ru(bpy)_3]^{2+}$ and metallotetraphenylporphyrin have been used as photosensitizers.[1,2] It is one of the most important points that visible light can be used in the conversion of solar energy. In this regard, metallophthalocyanines, which show strong absorption bands in the wavelength region from 600 to 700 nm, are attractive candidates for the photosensitizer. Water-soluble phthalocyanine and its magnesium(II) or zinc(II) complex were examined as photosensitizers.[3] Phthalocyanine complexes of magnesium(II), aluminum(III), zinc(II), and cadmium(II) were also employed as the photosensitizer in a solvent mixture of DMF and water.[4] It was further reported that those metal complexes with tetra-2,3-pyridinoporphyrazine showed photoredox activities in the solvent.[5]

We previously reported that a sandwich-type PcLnPcH complex (Pc denotes the phthalocyanine dianion) was oxidized to a radical PcLnPc$^\cdot$ species upon irradiation at $\lambda > 320$ nm in a solvent mixture of dichloromethane and acetonitrile.[6] Although the solubility of metallophthalocyanine complexes is usually very poor, a PcLnX complex (X denotes a monoanion) dissolves in common organic solvents such as methanol, acetone, or acetonitrile and also forms a relatively stable radical species depending upon the kind of X anions.[7] Thus, the lanthanoid(III) phthalocyanine complex, PcLnX, might be anticipated as a potential sensitizer for the photoredox system. In this paper, we report that the PcLnAcO complex (AcO denotes acetate anion) acts as the sensitizer for the photoreduction of methylviologen chloride ($MVCl_2$) in a methanol solution upon irradiation with visible light.

Experimental Section

Materials. The PcLnAcO complexes (Ln = Y(III), Sm(III), Gd(III), Yb(III), Lu(III)) were prepared according to the method described before:[8] the mixture of lanthanoid(III) acetate and phthalonitrile (1:8 mole ratio) was melted above 150 °C and was further heated at 200-230 °C for 2 h. The crude products (PcLnAcO, PcLnPcH, and decomposed organic compounds) were dissolved in DMF, and then the solution was poured on a silica gel column. The dark brown decomposed compounds accompanied by the PcLnPcH complex were at first eluted with methanol, following the blue PcLnAcO complex. The objective complex was obtained by concentration of the eluent and was confirmed by means of visible spectra and elemental analyses. $MVCl_2$ (Tokyo Kasei, reagent grade) and triethanolamine (TEOA) were used without further purification.

Apparatus. For steady-state irradiation, the sample solution in a glass cell with a 1-cm light path length was purged by argon gas and was irradiated with a 300-W tungsten lamp at 25 °C (the cell was situated 3 cm away from the light). The light with wavelength shorter than 440 nm was cut off by the use of a Toshiba Y-44 glass filter. The visible and fluorescence spectra were recorded on a Hitachi 200-20 spectrophotometer and a Hitachi 850 fluorescence spectrophotometer, respectively. Laser photolysis was carried out by using the second harmonics (532 nm, 100 ms) of a Quantel YG 580 Nd-YAG Q-switched laser. The details of the apparatus have been described elsewhere.[9]

* To whom correspondence should be addressed.
† Shimane University.
‡ Present address: Department of Chemistry, Faculty of Science, Nara Women's University, Nara 630, Japan.
§ Osaka University.

0020-1669/90/1329-0354$02.50/0